

1 Article

2 

# Moisture Content Measurement of Broadleaf Litters

  
3 

## using Near-Infrared Spectroscopy Technique

4 Ghiseok Kim <sup>1,3</sup>, Suk-Ju Hong <sup>1</sup>, Ah-Yeong Lee <sup>1</sup>, Ye-Eun Lee <sup>2</sup> and Sangjun Im <sup>2,3,\*</sup>5 <sup>1</sup> Department of Biosystems and Biomaterials Science and Engineering, Seoul National University, 1  
6 Gwanak-ro, Gwanak-gu, Seoul 08826, Republic of Korea; ghiseok@snu.ac.kr (G.K.); hsj5596@snu.ac.kr  
7 (S.H.); ayoung3308@snu.ac.kr (A.L.);8 <sup>2</sup> Department of Forest Sciences, Seoul National University, 1 Gwanak-ro, Gwanak-gu, Seoul 08826,  
9 Republic of Korea; dldpdms109@naver.com (Y.L.); junie@snu.ac.kr (S.I.)10 <sup>3</sup> Research Institute of Agriculture and Life Sciences, Seoul National University, 1 Gwanak-ro, Gwanak-gu,  
11 Seoul 08826, Republic of Korea; ghiseok@snu.ac.kr (G.K.); junie@snu.ac.kr (S.I.)

12 \* Correspondence: junie@snu.ac.kr; Tel.: +82-2-880-4759

13 **Abstract:** Near-infrared spectroscopy (NIRS) was implemented to monitor the moisture content of  
14 broadleaf litters. Partial least-squares regression (PLSR) models, incorporating optimal wavelength  
15 selection techniques, have been proposed to better predict the litter moisture of forest floor. Three  
16 broadleaf litters were used to sample the reflection spectra corresponding the different degrees of  
17 litter moisture. Maximum normalization preprocessing technique was successfully applied to  
18 remove unwanted noise from the reflectance spectra of litters. Four variable selection methods were  
19 also employed to extract the optimal subset of measured spectra for establishing the best prediction  
20 model. The results showed that the PLSR model with the peak of beta coefficients method was the  
21 best predictor among all candidate models. The proposed NIRS procedure is thought to be a suitable  
22 technique for on-the-spot evaluation of litter moisture.23 **Keywords:** near-infrared spectroscopy; multivariate analysis; partial least-squares regression; floor  
24 litter; optimal wavelength selection26 

### 1. Introduction

27 Floor litter refers to the relatively fresh organic residue on the uppermost layer of soil; it plays  
28 an important role in the water dynamics of the forest floor [1]. It can retain water within the layer  
29 during storm periods and deplete stored moisture through evaporation [2]. The moisture variation  
30 of litter can influence the hydrologic, carbon, and nutrient cycles of forests by altering the wetting  
31 and drying phases [3,4]. Moreover, litter moisture content is one of the critical determinants for fire  
32 ignition and spread in forests [5].33 Several attempts have been made to quantitatively measure the moisture variation of floor litter  
34 over the past couple of decades [6]. Among them, gravimetric method is the most common technique  
35 that determines the moisture amount from the difference in the litter weight of wet and dry  
36 conditions [7]. Yet it is a highly cumbersome and labor-intensive measurement.37 Some researchers have attested the continuous non-destructive techniques for litter moisture  
38 measurement. Gillespie and Kidd proposed the electrical impedance grids with mock leaf sensors to  
39 monitor leaf wetness of crops [8]. This technique was further improved by Hanson et al. [9]. On the  
40 other hand, time-domain reflectometry (TDR) probes have been employed in litter moisture  
41 measurement [10,11]. Ataka et al. developed a rather simple technique to continuously detect  
42 moisture content in litters using the modified capacitance sensors [1]. Robichaud and Bilskie  
43 developed a commercial device for measuring dead fuel moisture with a frequency domain (FD)  
44 sensor [12]. However, these methods exhibit inherently electrical bias and limitations for *in situ*  
45 measurement of litter moisture, because floor litter is highly heterogeneous and porous material with  
46 lower density and compactness.

47 Spectrometry has been adopted to analyze the quality of crops, chemicals and biomaterials.  
48 Near-infrared spectroscopy (NIRS) is a promising spectroscopic method that treats the near-infrared  
49 (NIR) region of an electromagnetic spectrum, which corresponds to the wavelength range of 750 to  
50 2,500 nm [13]. As a molecule has a different absorption frequency in the NIR region due to the  
51 vibrational patterns of chemical bonds (O-H, C-H, and N-H), NIRS can detect the special spectrum  
52 emitted from the intrinsic components of a test object. The frequency at which a certain vibration  
53 occurs is determined by the magnitude of bonds and mass of component atoms. A NIR device  
54 structurally consists of a light splitter, such as fiber optic cable, a monochromator, and a detector.  
55 Since this simple assembly is relatively easy to implement, NIRS is being widely used in  
56 nondestructive quality analysis for food, feed, pharmaceutical, and agricultural industries [14–16].

57 Sometimes NIRS technique is facing a serious difficulty in use. Spectral reflectance could be  
58 adulterated with the undesired environment and instrument causes. This undesired influence can  
59 reduce the detection accuracy of a prediction model. However, by applying suitable preprocessing  
60 techniques, the inappropriate information can largely be eliminated [17]. Preprocessing is a particular  
61 data analysis technique that eliminates unwanted noise for enhancing spectral features to clearly  
62 represent object characteristics. Rinnan et al. provided an overview of preprocessing techniques  
63 widely used in NIRS applications [18].

64 NIR spectra possess complex and overlapping absorption bands, so that mathematical  
65 procedures are needed for turning the spectra into meaningful information. Multivariate analysis  
66 refers to statistical procedure for analysis of data sets with more than one variable. It is capable of  
67 describing how the measured spectral features are related to the property of interest [19,20]. Until  
68 now, a number of multivariate techniques, such as partial least-squares regression (PLSR), principal  
69 component regression (PCR), and multiple linear regression (MLR), are commonly used to extract  
70 quantitative and qualitative information from NIR spectra [21,22].

71 Recently, considerable effort has been made in variable selection on multivariate data analysis.  
72 A highly correlated large spectrum can rather reduce the predictive ability of a model. Variable  
73 selection is a critical step to establish a reliable and robust model so it extracts a subset of spectral  
74 frequencies to produce better prediction results [23,24]. Many mathematical approaches for optimal  
75 wavelength selection have been derived from the scientific knowledge on the spectroscopic  
76 properties of samples [25].

77 In this study, we developed a non-contact technique to quantitatively monitor the moisture  
78 content of broadleaf litters using the NIRS. Floor litter samples were taken from deciduous forests,  
79 and gravimetric method was introduced to obtain the reference moisture content of litter samples.  
80 PLSR multivariate analysis has been employed to quantitatively predict the moisture content of floor  
81 litter. Four different methods were used to extract the optimal wavelength range through model  
82 development, and the model performance was also evaluated in conformity with variable selection  
83 methods.

## 84 **2. Materials and Methods**

### 85 *2.1. Litter Moisture Measurement*

86 The NIR spectra were acquired from the current year's litters, collected in the Seoul National  
87 University Arboretum in Seoul, Korea. The broadleaf litters were manually gathered under  
88 deciduous trees such as Chinese cork oak (*Quercus variabilis*), Sawtooth oak (*Quercus acutissima*), and  
89 Mongolian oak (*Quercus mongolica*). Sampled litters were first sorted to three types according to tree  
90 species, and each type of litter was separated into its 11 subsamples to represent different moisture  
91 conditions. All samples were immersed in water for 12 h in order to fully saturate, and then placed  
92 in a screened plate for a certain times to naturally drip water from samples. The reflectance spectra  
93 and litter moisture have been measured from three leaves of each sample at every one hour. The  
94 weight of each litter was immediately measured to obtain the wet weight of litter when NIR  
95 measurement was done. This process was repeated for all subsamples. After the experiment was  
96 completed, all litter samples were placed in an oven at a temperature of 70 °C for 48 h, and measured

97 the weight of oven-dried litter to obtain the dry weight. The moisture content of litter was calculated  
 98 based on the gravimetric method as follow:

$$\text{Moisture content}(\%) = \frac{w_w - w_d}{w_d} \times 100 \quad (1)$$

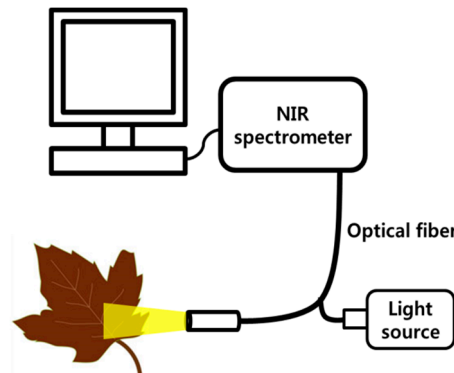
99 where  $w_w$  and  $w_d$  are the litter weight of wet and oven-dried conditions, respectively.

100 *2.2. NIR Spectra Measurement*

101 NIR reflectance spectra of litter samples were sampled in spectral range from 904 to 1,707 nm  
 102 with the NIR spectrometer (CDI-NIR128, Control Development Inc., USA). The tungsten-halogen  
 103 lamp (LS-1, Ocean Optics, USA) was installed as a light source as shown in Figure 1. The reflectance  
 104 spectrum was taken at three different positions on the litter surface, and then the averaged values  
 105 were recorded according to the moisture content of litter samples. The integration time was set to  
 106 0.25 s, and the distance between the sample and a probe was maintained at 1 cm. The reflectance of  
 107 the measured spectra was adjusted with white-referenced and dark-referenced spectra (Equation (2)).  
 108 The white-referenced spectrum was acquired from a white Teflon board, while the dark-referenced  
 109 was measured with a completely blocked fiber optic cable in a dark room.

$$\text{Reflectance}(\%) = \frac{S_i - D}{R - D} \times 100 \quad (2)$$

110 where  $S_i$  is the raw reflectance of the i-sample, and  $D$  and  $R$  represent the raw reflectance of dark-  
 111 and white-referenced spectra, respectively.



112

113 **Figure 1.** Schematic diagram of NIR spectra measurement.

114 *2.3. Multivariate Model Development*

115 The pretreatment of raw NIR spectra is the first step for model development and optimization to  
 116 achieve the better NIR veracity. The instrument and environment causes may lead to sample-to-  
 117 sample variations such as noise, light scattering, and optical path changes. Generally, spectral  
 118 preprocessing is strongly demanded to exclude noise components in reflectance spectra. In this study,  
 119 two scatter correction techniques (multiplicative scatter correction(MSC), standard normal  
 120 variate(SNV)), three normalization techniques (maximum normalization, mean normalization, range  
 121 normalization), and three Savitzky-Golay(SG) filters (smoothing, the first- and second-derivative  
 122 techniques) were used for spectra pretreatment.

123 The PLSR model was also employed to establish the relationship between litter moisture content  
 124 and reflectance characteristics. PLSR is a classical and widely used statistical method that bears a  
 125 relation between independent and dependent variables in large data sets. The general structure of  
 126 PLSR model is written as follow:

$$X = TP^T + E \\ Y = TQ^T + F, \quad (3)$$

127 where  $X$  is the  $n$  by  $m$  matrix of predictors,  $Y$  is the  $n$  by  $p$  matrix of responses,  $T$  is the  $n$  by 1 matrix  
 128 of the score matrix,  $E$  and  $F$  are error terms, and  $P$  and  $Q$  are the  $m$  by 1 and  $p$  by 1 loading matrices.

129 The performance of PLSR model is quantitatively assessed with the root mean square error  
 130 (RMSE) and the coefficient of determination ( $R^2$ ). For calibration purpose, the regression model with  
 131 a small RMSE value and a large value of  $R^2$  could be selected as an appropriate model. In this study,  
 132 latent variables (LVs) set with the smallest RMSE value was determined through the calibration and  
 133 validation procedures, and then the prediction model performance was evaluated through the  
 134 further test process.

135 A calibration model has to be evaluated with a validation set of samples to get an impression of  
 136 its predictive ability. Model test has sometimes conducted in the NIRS research to further ensure  
 137 model performance when the calibration and validation have completed. Among 99 spectra dataset,  
 138 model calibration, validation, and test have conducted from 60, 15, and 24 dataset, respectively. Both  
 139 preprocessing and regression analysis were done by using MATLAB commercial software (ver.  
 140 R2016, MathWorks, Natick, MA, USA).

#### 141 2.5. Optimal Wavelength Selection

142 The reflectance spectra, ranging 904 to 1,707 nm, were used in this study for establishing a  
 143 regression model to predict the moisture content of litter. PLSR technique generally uses the entire  
 144 range of wavelength's spectra, but recent studies have employed the most appropriate wavelength.  
 145 It proved that data analysis involving only a representative part of the spectra can lead to a better  
 146 prediction performance. Selection of optimal wavelength is to pick carefully the subset of spectral  
 147 data, which closely relate to the property of the interest. If the number of wavelength bands are  
 148 greater than that of spectral samples, the predictive model is likely to enhance its capability with the  
 149 optimal wavelength. In this study, various techniques such as the peak of beta coefficients, variable  
 150 importance in projection (VIP), bootstrap of beta coefficients, and interval PLS (iPLS) were applied to  
 151 determine the optimal wavelength from preprocessed spectra information.

##### 152 2.5.1. Peak of Beta Coefficient

153 The peak of beta coefficients (beta-peak method) extracts the optimal wavelength corresponding  
 154 to the peak of beta coefficients. The beta coefficient, the regression coefficient of PLSR model, is a  
 155 linear vector between the measured spectra and the predicted values. It measures the contribution of  
 156 each wavelength set on the model's predictive ability so as to select the optimum wavelength.

##### 157 2.5.2 Variable Importance in Projection

158 VIP is a method that evaluates the contribution of a variable on the weight matrix of a  
 159 multivariate analysis such as a PLSR model. It has been widely applied to determine major  
 160 wavelength bands when the variable matrix  $X$  defined in Equation (3) was considered [26]. Lohumi  
 161 et al. estimated how much the VIP value (Equation 4) could be influenced by the relationship between  
 162 the dependent variable matrix  $Y$  and the independent variable matrix  $X$  [27]:

$$v_j = \sqrt{\frac{p \sum_{a=1}^A [SS_a (w_{ak} / \|w_a\|^2)]}{\sum_{a=1}^A (SS_a)}}, \quad (4)$$

163 where  $v_j$  represents the VIP value,  $p$  is the number of variables,  $SS_a$  is the sum of squares explained  
 164 by the  $a^{\text{th}}$  component,  $w_a$  is the weight of  $a^{\text{th}}$  component, and  $w_{ak}$  is the weight of the  $a^{\text{th}}$  component at  
 165 the  $k^{\text{th}}$  variable.

166 The variable selection process by a VIP technique is terminated when the calculated VIP value  
 167 approaches to the threshold. In general, a threshold value of 1 is set in many studies[28]. In this study,  
 168 we compared the accuracies of developed models for selected wavelength sets by adjusting a  
 169 threshold value.

170 **2.5.3 Bootstrap of Beta coefficients**

171 The bootstrap of beta coefficients (bootstrap method) is a useful technique to set the confidence  
 172 interval, and estimate the significance level. It is mainly used when it is difficult to estimate the  
 173 distribution of samples. In the bootstrap method, a new dataset is first obtained by randomly re-  
 174 sampling the sample population. Thereafter, statistical values are obtained from the selected data  
 175 sets, and then the confidence interval is set [29]. The PLSR-bootstrap method can re-sample the  
 176 sample data  $n$  times and perform a PLSR for each re-sampled data set to obtain the beta coefficient.  
 177 From the distribution of beta coefficients, the confidence interval is obtained according to the  
 178 significance level of the beta coefficient of the specific variable. Finally, optimal wavelength is  
 179 determined by removing the variables with zero value in its confidence interval. The confidence  
 180 interval is computed by

$$I_k = \bar{b}_k \pm cs_k, \quad (5)$$

181 where  $I_k$  represents the confidence interval,  $\bar{b}_k$  is the mean of beta coefficients at the  $k^{\text{th}}$  variable,  $c$   
 182 is a constant that determines the confidence interval, and  $s_k$  is the standard deviation of beta  
 183 coefficients at the  $k^{\text{th}}$  variable.

184 In equation (5), the constant  $c$  is explicitly determined regarding the level of significance. A  
 185 higher significance level could select fewer wavelength bands. In this study, the number of re-  
 186 sampling is set to 1,000, and the model accuracy with the selected wavelength is evaluated by  
 187 changing the  $c$  values [30].

188 **2.5.4 Interval PLS**

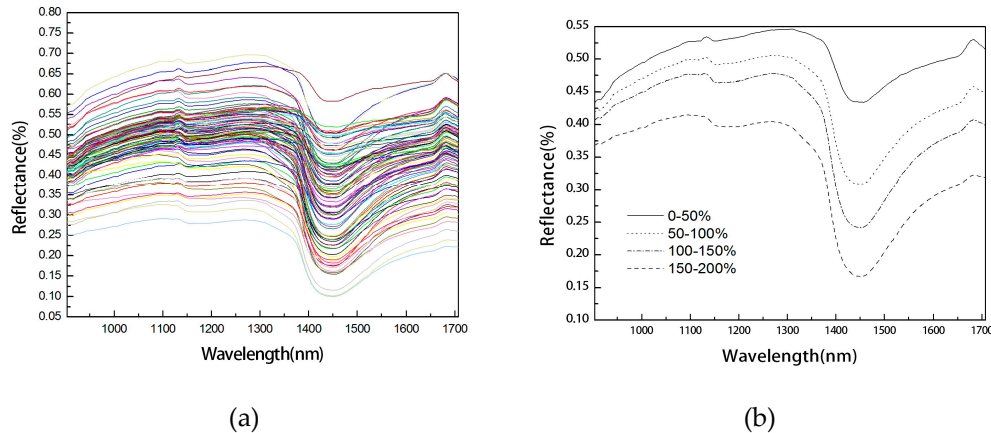
189 iPLS executes a PLSR model with the wavelength of a specific interval rather than the entire  
 190 wavelength band. It removes unnecessary wavelength bands and uses only the certain bands of a  
 191 given interval. The interval is repeatedly sampled to achieve the lowest RMSE value. In this study,  
 192 the entire wavelength band divided into 20 intervals and PLSR analysis was conducted to acquire the  
 193 optimal wavelength by shifting the wavelength range to the right or the left until the smallest RMSE  
 194 value was pursued [31].

195 **3. Results**

196 *3.1. Reflectance Spectra of Litters*

197 Figure 2 depicts the raw and average NIR reflectance spectra of litter samples in the wavelength  
 198 range of 900-1,700 nm prior to the pretreatment. There seems to be a slight variation in all reflectance  
 199 spectra through the litter moisture (Figure 2a). Figure 2b illustrates the averaged spectra with different  
 200 degrees of litter moisture (0–50%, 50–100%, 100–150%, and 150–200%). The spectral difference  
 201 appeared more clearly in Figure 2b. The absorption rate of NIR spectrum increased in the wavelength  
 202 range of 1,400–1,500 nm regardless of litter moisture. It is commonly known that NIR spectrum is  
 203 mostly absorbed at 980, 1,222, and 1,450 nm wavelength by the overtone and combination of the  
 204 vibrational transitions of water molecules [32]. On the NIR reflectance of litters, the absorption  
 205 coefficients at 980 and 1,222 nm wavelength were estimated to be less than  $1.3 \text{ cm}^{-1}$ , while the value  
 206 was estimated to be  $29.8 \text{ cm}^{-1}$  at a wavelength of 1,450 nm [32]. Figure 2b exhibits that the reflectivity

207 of NIR spectrum decreased sharply beyond the wavelength of 1,400 nm and had the lowest value at  
 208 the wavelength of 1,450 nm for all litter samples.



209

210

(a)

(b)

211  
212

**Figure 2.** Near-infrared reflectance spectrum of litter samples prior to preprocessing: (a) raw spectra; (b) averaged spectra.

213 *3.2. PLSR model for different preprocessing methods*

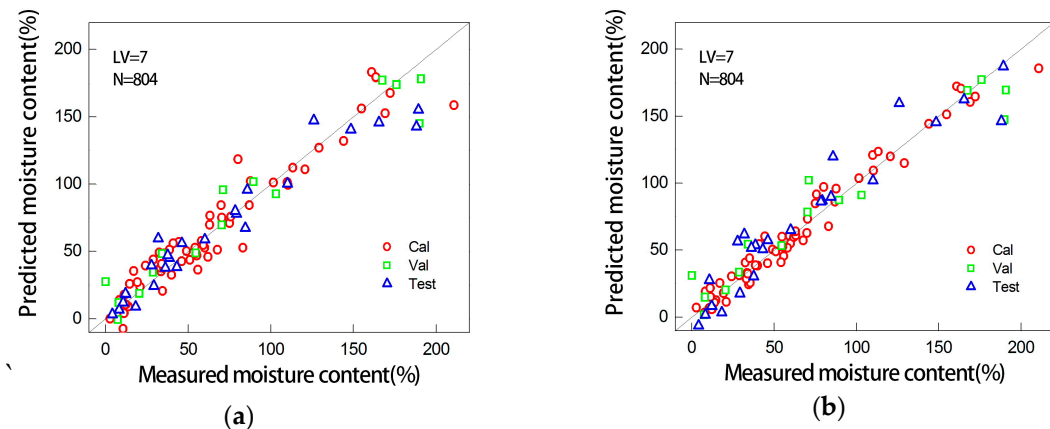
214 A number of pretreatment techniques for NIR spectra have been tested to achieve better  
 215 performance in litter moisture determination. Table 1 compares the results of PLSR model with  
 216 different spectral preprocessing techniques. The entire range of NIR dataset was treated and used to  
 217 develop PLSR models with the different preprocessing techniques. The performance of the model  
 218 was evaluated with two statistical criteria, coefficient of determination ( $R^2$ ) and root mean square  
 219 error (RMSE), between the reference and prediction of litter moisture content. The PLSR models  
 220 treated by the preprocessing methods of MSC, SNV, maximum normalization, and range  
 221 normalization have good prediction performance for validation. The test results of the models  
 222 showed that maximum normalization achieved the highest performance ( $R^2$ : 0.922, RMSE<sub>t</sub>: 15.711),  
 223 and followed by the model with range normalization preprocessing ( $R^2$ : 0.920, RMSE<sub>t</sub>: 15.970). Figure  
 224 3 shows the prediction result of two most highly correlated PLSR models for litter moisture  
 225 estimation.

226

**Table 1.** PLSR results with different preprocessing techniques.

Preprocessing Method	LVs	Calibration		Validation		Test	
		$R^2_c$	RMSE <sub>c</sub>	$R^2_v$	RMSE <sub>v</sub>	$R^2_t$	RMSE <sub>t</sub>
Raw data	9	0.930	12.757	0.920	19.041	0.884	19.170
SG smoothing	8	0.918	13.848	0.915	19.571	0.897	18.103
SG-1 <sup>st</sup> derivative	6	0.918	13.882	0.925	18.376	0.883	19.259
SG-2 <sup>nd</sup> derivative	6	0.937	12.114	0.913	19.792	0.840	22.506
MSC	8	0.926	13.132	0.933	17.432	0.914	16.482
SNV	8	0.927	13.069	0.943	16.106	0.915	16.426
Max. normalization	7	0.920	13.699	0.938	16.797	0.922	15.711
Mean normalization	9	0.926	13.149	0.926	18.308	0.892	18.479
Range normalization	7	0.922	13.535	0.931	17.722	0.920	15.970

227

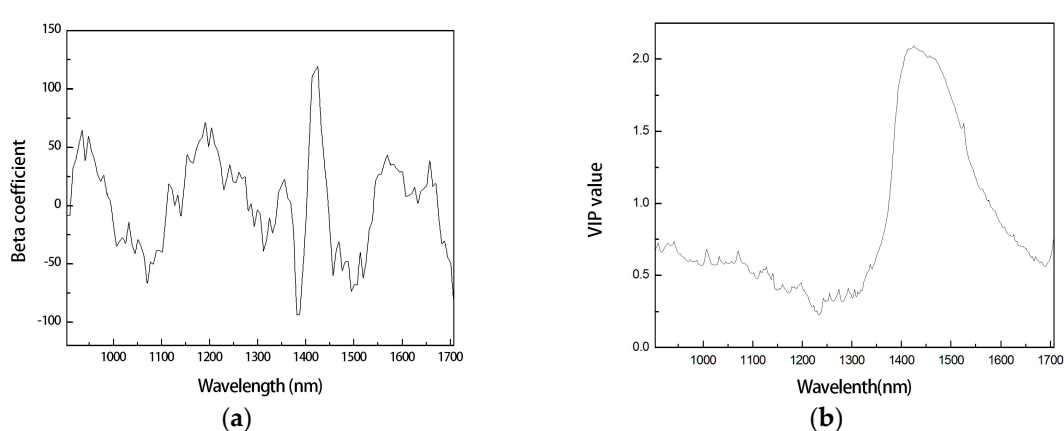


228      **Figure 3.** Comparison of predicted and measured moisture content. The prediction values were taken  
 229      from the PLSR model with (a) maximum normalization, and (b) range normalization preprocessing.

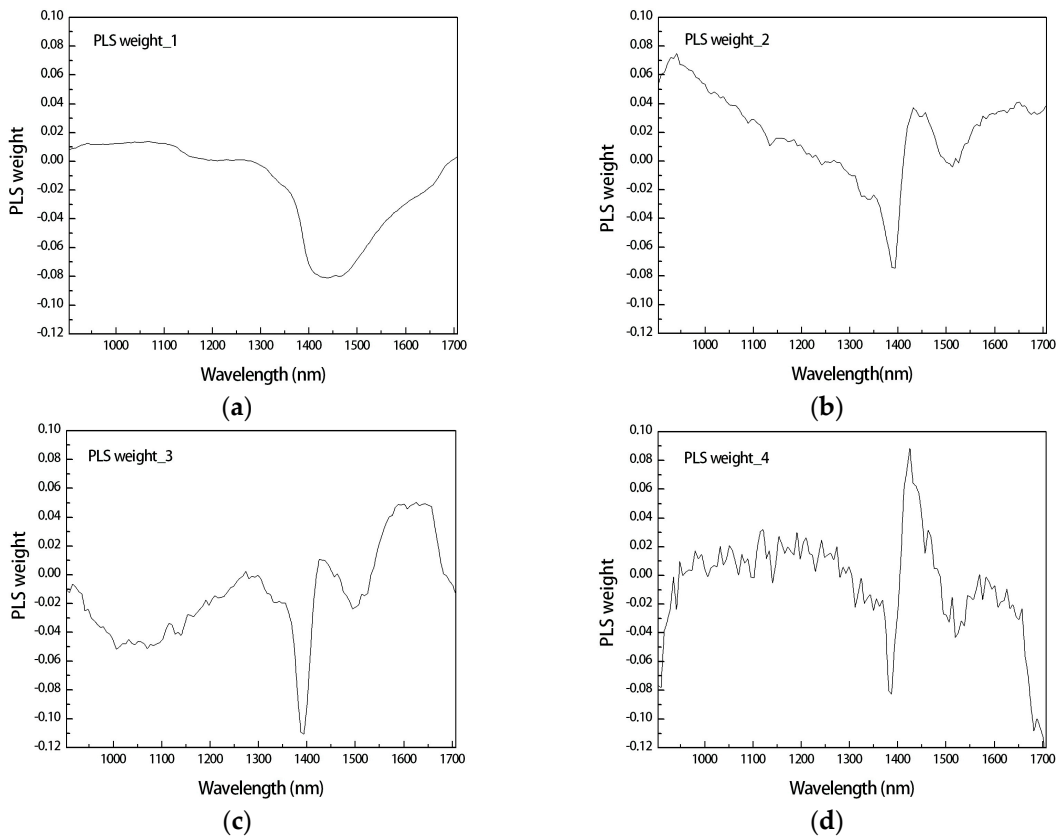
230      *3.3. PLSR models for optimal wavelength selection methods*

231      Four variable selection methods were used to set the optimal wavelength bands from around  
 232      800 data set of wavelength (900–1,700 nm). Maximum normalization was used as a pretreatment  
 233      technique through this step because the PLSR model incorporating maximum normalization  
 234      produced the highest performance in litter moisture estimation. The selected wavelength set was then  
 235      input the PLSR model for predicting the moisture content of floor litter. Figure 4 illustrates the beta  
 236      coefficients and VIP values of PLSR model derived from the entire wavelength's spectra. As shown  
 237      in Figure 4a, the peak points of beta coefficients were evenly distributed over the entire wavelength  
 238      band, and the largest peak point was discovered around 1,450 nm. But, large VIP values are observed  
 239      only in the range of 1,400–1,500 nm.

240      Figure 5 shows the first four weight vectors with respect to equivalent latent variables of the  
 241      PLSR model obtained from the entire wavelength's spectra. The weight vector can imply the  
 242      correlation between the measured spectrum and calculated latent variables through PLSR analysis.  
 243      It revealed how much the measured spectrum contributed to the formation of corresponding latent  
 244      variables. As shown in Figure 5a–d, the highest peak is observed around the wavelength of 1,400–  
 245      1,500 nm, which is highly correlated with the largest absorption coefficient of a water molecule.  
 246



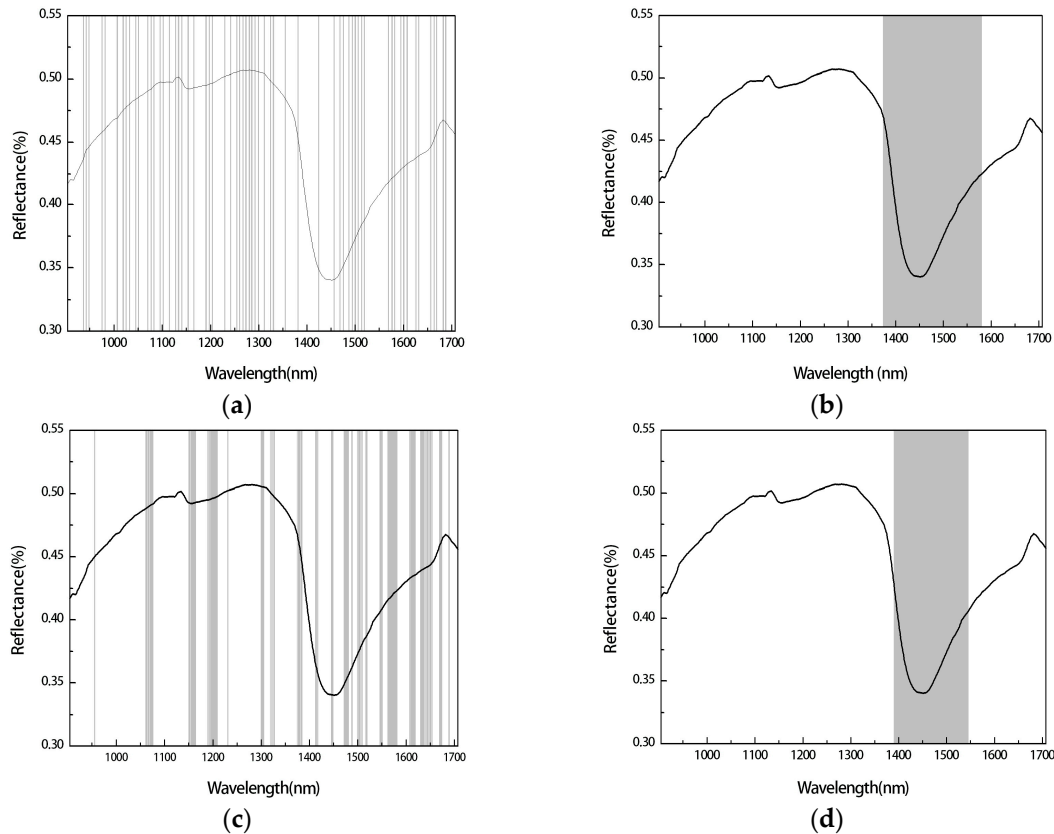
247      **Figure 4.** Beta coefficients (a) and VIP values (b) of the PLSR model with the entire wavelength's  
 248      spectra.



249  
250  
251 **Figure 5.** First four weight vectors with respect to equivalent latent variables of the PLSR model with  
the entire wavelength's spectra: (a) First weight vector; (b) Second weight vector; (c) Third weight  
vector; (d) Fourth weight vector.

252 Figure 6 shows the optimal wavelength bands determined by four variable selection methods.  
253 By applying the beta-peak method, 63 optimal wavelength bands corresponding to all peak points of  
254 the beta coefficient were selected, and they were uniformly distributed over the entire wavelength,  
255 as shown in Figure 6a. VIP method was implemented with different threshold values ( $v = 0.7, 1.0, 1.5,$   
256  $2.0$ ), and the wavelength ranged from  $1,375$  to  $1,577$  nm was finally selected for  $v = 1.0$  (Figure 6b). In  
257 the case of the bootstrap method, the significant level constant  $c$  was set to four cases ( $c = 1.0, 1.3, 1.6,$   
258  $1.9$ ). For  $c = 1.3$ , the extracted wavelength bands were relatively evenly distributed over the entire  
259 range, as shown in Figure 6c. After applying the iPLS technique with several intervals, 150 variables  
260 were selected in the wavelength range of  $1,394$ – $1,543$  nm (Figure 6d).

261  
262  
263  
264  
265  
266  
267  
268  
269



270  
271 **Figure 6.** Optimal wavelength derived by variable selection methods: (a) beta-peak ( $N = 63$ ); (b) VIP  
( $v = 1.0$ ,  $N = 203$ ); (c) bootstrap ( $c = 1.3$ ,  $N = 192$ ); (d) iPLS ( $N = 150$ ).

272 Table 2 presents the calibration, validation, and test performance of the PLSR models developed  
273 from the optimally selected wavelength's spectra. Predictive abilities of different models have been  
274 compared against the PLSR model with the entire wavelength's spectra (hereafter the full PLSR  
275 model). As 63 wavelength bands, selected by the beta-peak method, were input in the PLSR model,  
276 the model could better predict the litter moisture than the full PLSR model. The VIP method also  
277 confirmed that the performance of the PLSR model taken from the 316 spectra showed better  
278 prediction performance ( $R^2$ : 0.923,  $RMSE_t$ : 15.597) than that of the full PLSR\_model. VIP value of 1.5  
279 marked 150 wavelength set among the entire wavelength range, and had a similar ability for litter  
280 moisture estimation ( $R^2$ : 0.920,  $RMSE_t$ : 15.916) with the entire wavelength PLSR\_model.

281 The bootstrap method was applied to select the optimal wavelength. The PLSR model with 305  
282 spectra data ( $c = 1.0$ ) showed better capability in data analysis ( $R^2$ : 0.927,  $RMSE_t$ : 15.164), while the  
283 PLSR model with 106 spectra ( $c = 1.6$ ) also showed similar prediction performance ( $R^2$ : 0.918,  $RMSE_t$ :  
284 16.128) when compared to the full PLSR model. A total of 150 wavelength bands was optimally  
285 selected in the iPLS technique application, and the prediction performance of PLSR model achieved  
286 the  $R^2$  value of 0.918,  $RMSE_t$  value of 16.115.

287 As presented in Table 2, the predictive abilities of the PLSR models with reduced wavelength  
288 bands by employing the variable selection methods showed similar or better performance with the  
289 full PLSR\_model, excepting only two cases of VIP ( $v = 2.0$ ) and bootstrap method ( $c = 1.9$ ). But, optimal  
290 wavelength selection can improve the prediction accuracy by effectively identifying the best subset  
291 of candidate spectra. It also eliminates unnecessary information so as to enhance the efficiency and  
292 effectiveness of model run. Figure 7 shows the prediction results of the best PLSR models, which  
293 were derived from the optimally selected wavelength's spectra.

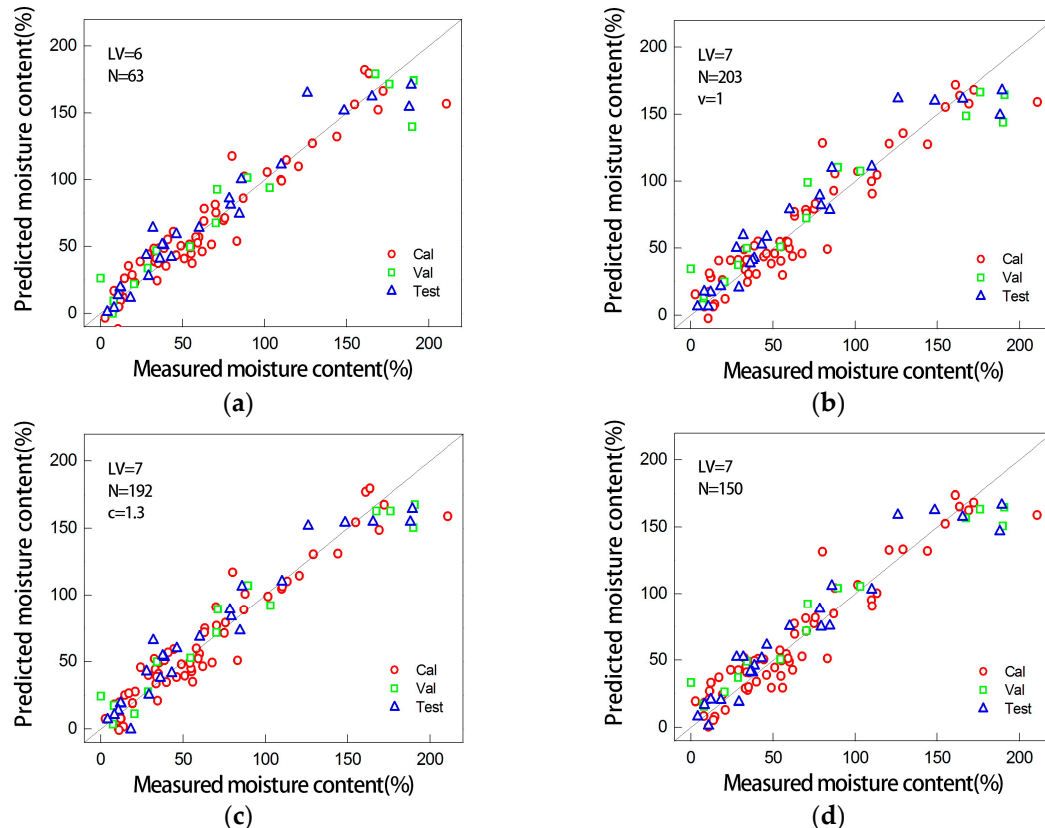
294  
295  
296  
297

298

**Table 2.** PLSR performance comparison with variable selection methods.

Method	LVs	No. of Variables	Calibration		Validation		Test	
			$R_c^2$	$RMSE_c$	$R_v^2$	$RMSE_v$	$R^2$	$RMSE_t$
Full PLSR	7	804	0.920	13.699	0.938	16.797	0.922	15.711
iPLS	7	150	0.900	17.825	0.930	17.825	0.918	16.115
VIP	$v = 0.7$	7	0.924	13.391	0.934	17.276	0.923	15.597
	$v = 1.0$	7	0.905	20.131	0.910	20.131	0.918	16.130
	$v = 1.5$	7	0.909	14.620	0.926	18.314	0.920	15.916
	$v = 2.0$	7	0.884	16.522	0.853	25.818	0.859	21.167
Boots	$c = 1.0$	7	0.919	13.795	0.941	16.392	0.927	15.164
-trap	$c = 1.3$	7	0.916	14.012	0.940	16.472	0.924	15.526
	$c = 1.6$	7	0.909	14.586	0.929	17.954	0.918	16.128
	$c = 1.9$	7	0.875	17.1670	0.884	22.913	0.878	19.655
Beta-peak	6	63	0.918	13.834	0.932	17.494	0.930	14.905

299

**Figure 7.** Comparison of the PLSR results with variable selection methods: (a) beta-peak; (b) VIP; (c) bootstrap; (d) iPLS.300  
301302 **4. Conclusions**

303 Litter refers to the organic residue on the forest floor, and plays an important role in forest water  
 304 cycle. Litter moisture is one of the critical determinants for evaporation, infiltration, and fire ignition  
 305 in a forest environment. In this study, the commonly used technique, NIRS, has been implemented  
 306 to fast, non-destructively monitor the moisture content of broadleaf litters. Several techniques for

307 data pretreatment and optimal wavelength selection have been tested to establish a reliable and  
308 robust multivariate model.

309 Prior to establishing a PLSR model, the pretreatment was conducted to eliminate the unwanted  
310 noise in raw NIR spectra. Maximum normalization preprocessing, one of well-known normalization  
311 techniques, achieved the best prediction ability in litter moisture estimation among 8 pretreatment  
312 methods. The entire wavelength may uphold the whole information of target samples, but the  
313 redundant data causes the decline in model accuracy. The peak of beta coefficients seems to be the  
314 best variable selector to extract the optimal wavelength bands as to yield the better predictive ability  
315 in litter moisture estimation.

316 The NIRS has been commonly used in both qualitative and quantitative analysis of target  
317 samples with respect to the vibrational energy of molecules. The low optical absorbance  
318 characteristics of NIR rays facilitates deeper penetration than mid-infrared rays. This optical method  
319 has some merits in reducing time-consuming work and supporting reliable results by minimizing the  
320 errors that may originate from the quick changes of litter moisture on the spot.

321 The NIRS has also limited ability to resolve noise that is caused by the instrument and  
322 environment causes. NIR spectra tends to be highly complex and over-parameterized, which  
323 sometime yields a poor prediction. In the face of its drawback, multivariate analysis through variable  
324 reduction and proper pretreatment have been successfully introduced in practical uses. It is believed  
325 that this research provides with great opportunities for multicomponent analysis of agricultural  
326 products and foods, as well as many other scientific sectors, such as life sciences and biomaterial  
327 research.

328 **Acknowledgments:** This research was supported by Basic Science Research Program through the National  
329 Research Foundation of Korea (NRF) funded by the Ministry of Education (NRF-2015R1D1A1A02061769).

330 **Author Contributions:** G.K. designed the experimental concept and data analysis methods; S.H and A.L.  
331 performed experiments and analyzed the data; Y.L supported experiments and data analysis; S.I. wrote the  
332 article and have been supervising, discussing the experiments and edited the presented work.

333 **Conflicts of Interest:** The authors declare no conflict of interest.

### 334 **References**

- 335 1. Ataka, M.; Kominami, Y.; Miyama, T.; Yoshimura, K.; Jomura, M.; Tani, M. Using capacitance sensors for  
336 the continuous measurement of the water content in the litter layer of forest soil. *Appl. Environ. Soil Sci.*  
337 2014, ID627129. Doi:dx.doi.org/10.1155/2014/627129
- 338 2. Stocks, J.B. Moisture in the forest floor - its distribution and movement. Dept. of Fisheries and Forestry,  
339 Canadian Forestry Service, 1970, No. 1271. p. 20.
- 340 3. Xiao, Q.; McPherson, E.G. Surface water storage of twenty tree species in Davis, California. *J. Environ. Qual.*,  
341 2016, 45, 188–198. Doi:10.2134/jeq2015.02.0092
- 342 4. Borken, W.; Matzner, E. Reappraisal of drying and wetting effects on C and N mineralization and fluxes in  
343 soils. *Glob. Change Biol.*, 2009, 15, 808–824.
- 344 5. Johnson, E.A.; Miyanishi, K. *Forest Fires: Behavior and Ecological Effects*; Academic Press: Washington, DC,  
345 USA, 2001, p. 594.
- 346 6. Schunk, C.; Ruth B.; Leuchner, M.; Wastl, C.; Menzel, A. Comparison of different methods for the in situ  
347 measurement of forest litter moisture content. *Nat. Hazard Earth Sys.*, 2016, 16, 403–415. doi:10.5194/nhess-  
348 16-403-2016.
- 349 7. Wotton, B.M.; Stocks, B.; Martell, D.L. An index for tracking sheltered forest floor moisture with the  
350 Canadian Forest Fire Weather Index System. *Int. J. Wildland Fire*, 2005, 14, 169–182. Doi:10.1071/WF04038
- 351 8. Gillespie, T.J.; Kidd, G. Sensing duration of leaf moisture retention using electrical impedance grids. *Can. J.*  
352 *Plant Sci.*, 1978, 58, 179–187
- 353 9. Hanson, P.J.; O'Neill, E.G.; Chambers, M.L.S.; Riggs, J.S.; Joslin, J.D.; Wolfe, M.H. Soil respiration and litter  
354 decomposition. In *North America Temperate Deciduous Forests Response to Changing Precipitation Regimes*;  
355 Hanson, P.J.; Wullschleger, S.D., Eds.; Springer: New York, USA, 2003, pp 163–189.

356 10. Borner, T.; Johnson, M.G.; Ryglewicz, P.T.; Tingey, D.T.; Jarrell, G.D. A two-probe method for measuring  
357 water content of thin forest floor litter layers using time domain reflectometry. *Soil Technol.*, **1996**, *9*, 199–  
358 207

359 11. Pumpanen, J.; Ilvesniemi, H. Calibration of time domain reflectometry for forest soil humus layers. *Boreal  
360 Environ. Res.*, **2005**, *10*, 589–595

361 12. Robichaud, P.R.; Bilskie, J. A new tool for fire managers—an electronic duff moisture meter. *Fire Management  
362 Today*, **2004**, *64*, 15–18.

363 13. American Society for Testing and Materials, E1866-97: Standard Guide for Establishing Spectrophotometer  
364 Performance Tests, and E1655: Standard practices for infrared, multivariate, quantitative analysis, Official  
365 ASTM Publications, Philadelphia, PA, **2000**.

366 14. Choe, E.; van der Meer, F.; van Ruitenbeek, F.; van der Werff, H.; de Smeth, B.; Kim, K.W. Mapping of  
367 heavy metal pollution in stream sediments using combined geochemistry, field spectroscopy, and  
368 hyperspectral remote sensing: a case study of the Rodalquilar mining area, SE Spain. *Remote Sens. Environ.*,  
369 **2008**, *112*, 3222–3233.

370 15. Choi, C.H.; Lee, K.J.; Park, B.S. Prediction of soluble solid and firmness in apple by visible/near-infrared  
371 spectroscopy. *J. Korean Society for Agricultural Machinery*, **1997**, *22*, 256–265. (In Korean)

372 16. Lu, R.F.; Guyer, D.E.; Beaudry, R.M. Determination of firmness and sugar content of apples using near-  
373 infrared diffuse reflectance. *J. Texture Stud.*, **2000**, *31*, 615–630.

374 17. Porep, J.U.; Kammerer, D.R.; Carle R. On-line application of near infrared (NIR) spectroscopy in food  
375 production. *Trends in Food Science & Technology*, **2015**, *46*, 211–230.

376 18. Rinnan, A°; Berg, F. van den; Engelsen, S.B. Review of the most common pre-processing techniques for  
377 near-infrared spectra. *Trends in Analytical Chemistry*, **2009**, *28*, 1201–1222.

378 19. Kim, Y.T.; Suh, S.R. Comparison of performance of models to predict hardness of tomato using  
379 spectroscopic data of reflectance and transmittance. *J. Biosystems Eng.*, **2008**, *33*, 63–68. (In Korean)

380 20. Kawano, S.; Watanabe, H.; Iwamoto, M. Determination of sugar content in intact peaches by near infrared  
381 spectroscopy. *J. Japan. Soc. Hort. Sci.*, **1992**, *61*, 445–451.

382 21. Dull, G.G.; Leffler, R.G.; Birth, G.S.; Smittle, D.A. Instrument for non-destructive measurement of soluble  
383 solids in honeydew melons. *Trans. Am. Soc. Agric. Eng.*, **1992**, *35*, 735–737.

384 22. Chung, H.-I.; Kim, H.-J. Near-infrared spectroscopy: Principles. *Anal. Sci. Technol.*, **2000**, *13*, 138–151.

385 23. Sarathjith ,M.C; Das, B. S; Wani, S.P; Sahrawat, K.L. Variable indicators for optimum wavelength selection  
386 in diffuse reflectance spectroscopy of soils, *Geoderma*, **2016**, *267*, 1–9.

387 24. Zhang, C; Jiang, H; Liu, F; He, Y. Application of Near-Infrared Hyperspectral Imaging with Variable  
388 Selection Methods to Determine and Visualize Caffeine Content of Coffee Beans. *Food and Bioprocess  
389 Technology*, **2017**, *10*, 213–221.

390 25. Fernández Pierna, J.A; Abbas, O; Baeten, V; Dardenne, P. A backward variable selection method for PLS  
391 regression (BVSPLS). *Analytica Chimica Acta*, **2009**, *642*, 89–93.

392 26. Anderson, C.M.; Bro R. Variable selection in regression—a tutorial. *J. Chemometric.*, **2010**, *24*, 728–737.

393 27. Lohumi, S.; Lee, S.; Cho, B.-K. Optimal variable selection for Fourier transform infrared spectroscopy  
394 analysis of starch-adulterated garlic powder. *Sensor. Actuator. B*, **2015**, *216*, 622–628.

395 28. Mehmood, T. et al. A review of variable selection methods in partial least squares regression. *Chemometric.  
396 Intell. Lab.*, **2012**, *118* 62–69.

397 29. Bickel, P.J.; Freedman, D.A. Some asymptotic theory for the bootstrap. *Ann. Stat.*, **1981**, *9*, 1196–1217.

398 30. Lazraq, A. et al. Selecting both latent and explanatory variables in the PLS1 regression model. *Chemometric.  
399 Intell. Lab.*, **2003**, *66*, 117–126.

400 31. Norgaard, L. et al. Interval partial least-squares regression (iPLS): a comparative chemometric study with  
401 an example from near-infrared spectroscopy. *Appl. Spectrosc.*, **2000**, *54*, 413–419.

402 32. Collins, J.R. Change in the infra-red absorption spectrum of water with temperature. *Phys. Rev.*, **1925**, *26*,  
403 771–779.

404